# Heat Transfer in Packed and Fluidized Beds by the Method of Cyclic Temperature Variations

**GEORGE C. LINDAUER**
**Brookhaven National Laboratory, Upton, New York**

Particle-to-gas heat transfer coefficients were determined in packed and fluidized beds with large diameter particles and high mass velocities using the cyclic temperature method.

Experimental results for packed beds were satisfactorily correlated within 10% deviation as $\varepsilon j_h$ vs. $N_{Re}$ and were found to compare favorably with results of other experimenters obtained with much lower mass velocities and larger particles. The particle-to-gas heat transfer coefficient varied as $G^{0.60}$ for the steel spheres vs. $G^{0.66}$ for the tungsten spheres, and as $D_p^{-0.44}$.

Heat transfer coefficients obtained at minimum fluidization were in good agreement with those obtained with packed beds. As the mass velocity was increased above that required for minimum fluidization, heat transfer coefficients remained essentially constant.

In packed beds or fluidized beds of spherical particles generating heat at a constant rate and cooled by fluid flowing through the bed, it is necessary to know the average value of particle-to-fluid heat transfer coefficient to calculate the particle surface area required to maintain a specified maximum temperature difference between the fuel surface and the cooling gas at the exit of the bed. In correlating particle-to-fluid heat transfer coefficients, it is generally assumed that either the Nusselt number or $j_h$ is a function of Reynolds number.

Recent reviews of the literature by Barker (*1*, *2*) and Frantz (*3*) indicate wide variations in the experimental data relating $j_h$ and $N_{Re}$. Little experimental work has been performed with very high mass velocities in packed or fluidized beds or with small diameter particles in packed beds. The purpose of this study was to accurately determine particle-to-gas heat transfer coefficients in gas flow through packed and fluidized beds over a wide range of $N_{Re}$ with particular emphasis on small diameter particles and high mass flow rates.

The method of cyclic temperature variations was used to determine the particle-to-coolant heat transfer coefficient. In these experiments, a sinusoidal temperature variation with respect to time was induced in the gas prior to its passage through the particulate bed. As a result of heat exchange between the particles and the gas, the sinusoidal temperature wave in the gas after passage through the bed was reduced in amplitude and exhibited a shift in phase. The heat transfer coefficient was calculated from the amplitude and phase relationships of the wave, the thermal properties of gas and particles, the geometry, and the coolant flow rate. Advantages of this method include:

1. The particle surface temperature need not be measured.
2. Power requirements are small because only small temperature changes are required.
3. The experiment is run under nearly isothermal conditions.

## REVIEW OF THE LITERATURE

Schumann (*4*) initiated the use of transient response techniques in determining heat transfer coefficients when he theoretically investigated the effect of introducing a step change in temperature into a fluid at the inlet of a packed bed. His graph of the outlet coolant temperature vs. time for different heat transfer coefficients could be used in conjunction with experimental data to evaluate the heat transfer coefficient.

The transient response method was simplified greatly by Bell and Katz (*5*) in their analysis of a packed-bed system in which the inlet fluid temperature was varied sinusoidally when they determined that the particle-to-fluid heat transfer coefficient could be calculated from the coolant temperatures measured simultaneously upstream and downstream of the bed. Dayton et al. (*6*) extended the theory to encompass particles with a low thermal conductivity. Dingee and Chastain (*7*), as well as Dayton et al. (*6*) discussed magnitudes of errors which might arise from coolant mixing and from variations in velocity and heat transfer coefficient. Ball (*8*) used the cyclic temperature method to determine the effective radial and axial thermal conductivities of the bed as well as the particle-to-fluid heat transfer coefficient. Results of experiments in packed beds performed by Meek (*9*), Kim (*10*), and Gates (*11*) tended to confirm the validity of the cyclic temperature method for packed beds.

Both Kim (*10*) and Littman and Stone (*12*) have previously used the cyclic temperature technique to determine heat transfer experiments in fluidized beds. Kim (*10*) introduced a sinusoidal temperature wave into the inlet gas and measured the amplitude ratio and phase shift at several positions in a deep fluidized bed with thermocouples. His results indicated that complete damping of amplitude occurred within 0.25 in. of the upstream support and that a uniform solid and gas temperature existed in the remainder of the bed. He based the correlation of his results on a two-zone model, that is, a decaying zone close to the upstream bed support and a constant-temperature zone in the remainder of the bed. Littman and Stone (*12*) introduced a square wave in the inlet gas of a deep fluidized bed and used a thermocouple in the exit gas to measure the amplitude ratio and phase shift between the inlet and outlet gas. To interpret their results, they assumed plug flow in the gas and an infinite solids mixing rate. Because a deep bed was used, $L/D_p \approx 57$, only minimum values of the heat transfer coefficient could be obtained.

## THEORY

The differential Equations (1) and (2), which in the present experiments were used to relate the heat transfer coefficient to the particle and fluid temperature, are based on the following assumptions.

1. The system is linear and hence the differential equations and the solution are also linear.
2. The bed void fraction is constant.
3. Fluid velocity profile is uniform across the bed.
4. There is no longitudinal dispersion of heat due to particle conduction or gas mixing and there are no radial temperature gradients.
5. Physical properties of the fluid and bed are constant.
6. The particle-to-fluid heat transfer coefficient is constant throughout the bed.
7. Thermal conductance of a particle is large compared with the particle-to-fluid heat transfer coefficient.

These assumptions will be treated in more detail in the discussion.

$$\frac{D_p \varepsilon}{6(1-\varepsilon)} \rho_g C_g \left( \frac{\partial T_g}{\partial t} + V \frac{\partial T_g}{\partial X} \right) = h(T_s - T_g) \tag{1}$$

$$\frac{-D_p}{6} \rho_s C_s \frac{\partial T_s}{\partial t} = h(T_s - T_g) - \frac{D_p K_e}{6(1-\varepsilon)} \frac{\partial^2 T_s}{\partial X^2} \tag{2}$$

Explicit solutions of Equations (1) and (2) for $N_{St}$ in terms of the amplitude ratio and the phase displacement of the downstream wave compared with the upstream wave have not been determined, although Kim (*10*) has reduced these equations to two nonlinear simultaneous algebraic equations. For the limiting case of infinitely large $K_e$, Bell and Katz (*5*) and later Littman and Stone (*12*) solved Equations (1) and (2) explicitly for the heat transfer coefficient. For $K_e = 0$, the solutions for $N_{St}$ in terms of the amplitude ratio $(T_{g_1}/T_{g_2})$ and the phase displacement of the downstream wave compared with upstream are

$$N_{St} = \frac{y^2 \left[ 1 \pm \sqrt{1 - \left( \dfrac{D_p \varepsilon}{3y(1-\varepsilon)L} \ln \dfrac{T_{g_1}}{T_{g_2}} \right)^2} \right]}{\dfrac{D_p}{3(1-\varepsilon)L} \ln \dfrac{T_{g_1}}{T_{g_2}}} \tag{3}$$

and

$$N_{St} = \frac{y}{\varepsilon} \sqrt{\frac{\left[ \dfrac{\omega}{V\varepsilon} - \dfrac{\varphi}{L} \right] \left[ \dfrac{D_p \varepsilon}{6(1-\varepsilon)} \right]}{- \left[ y + \left\{ \dfrac{\omega}{V\varepsilon} - \dfrac{\varphi}{L} \right\} \left\{ \dfrac{D_p \varepsilon}{6(1-\varepsilon)} \right\} \right]}} \tag{4}$$

where $N_{St} = (h/C_g G)$, $\varphi$ is the phase shift in radians, and

$$y = \frac{C_s \rho_s D_p \omega \varepsilon}{6 C_g G}$$

## APPARATUS

A schematic diagram of the apparatus is shown in Figure 1. Air was supplied from four 94 cu. ft. tanks at 250 lb./sq. in. Constant flow was achieved by a flow controller which could be set to give any pressure up to 175 lb./sq. in. gauge. Steady mass flow rates up to 100,000 lb./(hr.)(sq. ft.) could be obtained through the 1-in. square test section. A 6-in. long calming section made up of a bed of $\frac{1}{8}$ in. spheres was located upstream of the heater and two 250-mesh stainless steel screens were placed upstream of the bed. Air flow rates were measured by rotameters with an overall range of 0.2 to 150 std. cu. ft./min.

A 400-mesh stainless steel wire-screen electrical resistance heater was used to produce the sinusoidal gas temperature variation. The 0.001-in. diameter wire enabled a fast response to be obtained. Power generation and input was uniform across the test section. Eight screens spaced 0.1 in. apart were used in series to produce the desired overall resistance. A variable frequency oscillator (0.01 to 100 cycles/sec.) was used to generate a sinusoidal signal which was then amplified and passed through the heater. A peak power of 750 w. could be delivered uniformly to the air stream with a peak voltage of 25 v.

Air temperatures immediately upstream and 1 in. downstream of the bed were measured with resistance thermometers made up with approximately 1 ft. of 0.001-in. diameter platinum wire. The wire was woven through a 250-mesh nylon screen and traversed 70% of the area of the central region of the test section. Each resistance thermometer comprised one leg of a Wheatstone bridge balanced at the mean thermometer resistance. The out-of-balance currents which were linear with resistance change were amplified and recorded on a two-channel oscillograph. A resistance box was substituted for the resistance thermometer to determine the current obtained for a specified resistance change and so ob-

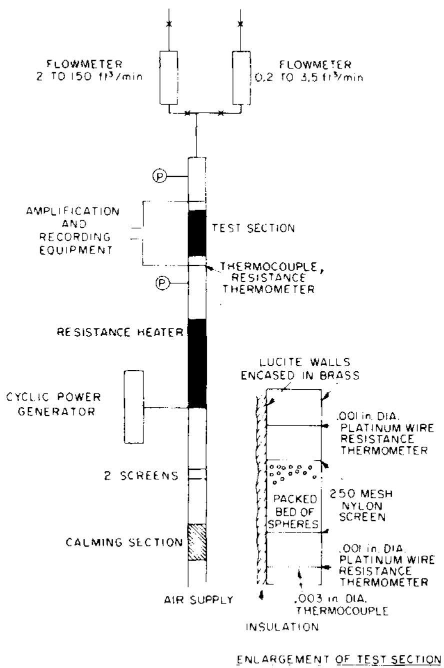


**Fig. 1. Schematic diagram of experimental apparatus.**

tain the ratio of the sensitivities of the thermometer amplifier systems.

The packed bed of spheres was sandwiched between two nylon screens in the 1-in. square test section. The test section was 6 in. long and was supported in a 0.25-in. thick Lucite frame with a brass outer shell encased in 2 in. of Fibrefrax insulation.

## PRELIMINARY TESTING

Preliminary testing of the apparatus without a bed of particles was performed to determine the response of the resistance thermometer to the cyclic power generation. At a cycling rate of 10 cycles/sec. and a gas mass flow rate of 60,000 lb./(hr.)(sq. ft.) the temperature amplitude recorded was 70% of that at 0.1 cycles/sec. The upstream and downstream resistance thermometers measured identical temperature changes over the entire range of flows and frequencies used in these experiments.

When the apparatus was operated with a fluidized bed, the interaction of the impressed sine wave and the fluidized bed system introduced random noise in the output wave. This problem was overcome by filtering electronically the random noise from the output signal.

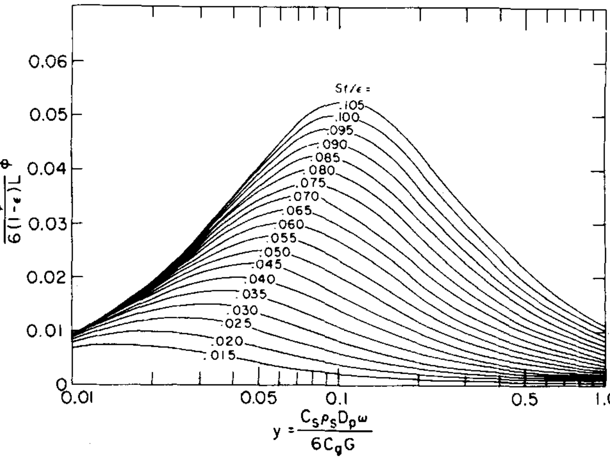


**Fig. 3. Theoretical variation of phase shift with frequency.**

## DESIGN OF EXPERIMENTS

Heat transfer coefficients in the packed bed experiments were determined from Equations (3) and (4). When Equation (3) is used to determine $N_{St}$ from the amplitude ratio $(T_{g_1}/T_{g_2})$, two possible mathematical solutions seem possible. Under typical experimental conditions, where $\frac{D_p}{3(1-\varepsilon)Ly}\ln\frac{T_{g_1}}{T_{g_1}}$ is small, one solution shows $N_{St}$ varying with frequency and gives $N_{St}$ more than an order of magnitude too large. The other solution which gives $N_{St}$ invariant with frequency reduces to

$$N_{St} = \frac{D_p}{6(1-\varepsilon)L}\ln\frac{T_{g_1}}{T_{g_2}}\left[1+\frac{D_p}{6(1-\varepsilon)Ly}\ln\frac{T_{g_1}^2}{T_{g_2}}+\ldots\right] \quad (5)$$

and is taken as the one having physical meaning.

An important feature of the cyclic temperature method is that although the heat transfer coefficient is independent of frequency, the amplitude ratio and phase shift obtained are very dependent on frequency. This is illustrated by Figures 2 and 3 which are parametric studies of the variations of amplitude ratio and phase shift as a function of $y$, where $y$ is proportional to $\omega$.

Determination of heat transfer coefficients at low frequencies requires extremely accurate measurements, since for this condition the amplitude ratio and phase angle vary only slightly with changes in $N_{St}$. At very high frequencies, the amplitude ratio becomes independent of frequency and the heat transfer coefficient can be accurately obtained from amplitude ratio measurements. At intermediate frequencies, the heat transfer coefficient can be accurately obtained from the phase lag of the downstream temperature wave. In fact, both $N_{St}$ and $y$ can be obtained if a number of frequency runs are made in the region where the maximum phase shift occurs.

Whenever possible, experiments were performed at frequencies where the greatest accuracy in determining $N_{St}$ could be obtained. When the amplitude ratio was determined, frequencies high enough so that $N_{St}$ approached $\frac{D_p}{6(1-\varepsilon)L}\ln\frac{T_{g_1}}{T_{g_2}}$ were used. At very high mass flow rates this required frequencies in excess of 10 cycles/sec. When the $N_{St}$ was obtained from the phase angle, suitable frequencies were used to give the maximum phase angle.

Heat transfer coefficients for the fluidized beds were calculated with several methods. Since $K_e$ was not known, for each experimental run, calculations were performed using Equations (3) and (4) for $K_e = 0$ and equations derived by Bell and Katz (*3*) for $K_e$ infinitely large. In addition, for a number of runs the nonlinear simultaneous equations of Kim (*10*) were solved for $N_{St}$ in terms of the amplitude ratio using intermediate values of $K_e$ by means of a computer code. The $N_{St}$ calculated using $K_e$ from zero to infinitely large values were compared and in all runs they differed by less than 15% because of the nature of the solutions to the differential equations for the high frequencies required in the experiments. Therefore, for uniformity, in presenting the results an infinite solids mixing rate was used exclusively.

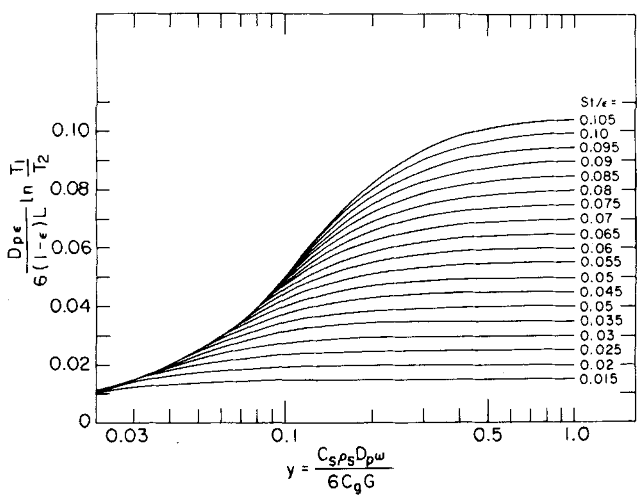


**Fig. 2. Theoretical variation of amplitude ratio with cyclic frequency.**

## PACKED BEDS

Results are given in Table 1* and are plotted as $h$ vs. $G$ in Figure 4 and as $\varepsilon j_h$ vs. $N_{Re}$ in Figure 5. The ordinate of Figure 5 was selected as $\varepsilon j_h$ since a number of experimenters have found that $j_h$ varies with $\varepsilon$.

Experiments were performed using beds of uniform steel spheres with particle diameters of 0.03935, 0.069, and 0.125 in. and using beds of tungsten spheres with average

*Deposited as document 9645 with the American Documentation Institute, Photoduplication Service, Library of Congress, Washington 25, D.C., and may be obtained for $1.25 for photoprints or 35-mm. microfilm.

particle diameters of 0.019 in. The beds used were shallow with a minimum $L/D_p$ of 5.25 and a maximum $L/D_p$ of 12.9. This restriction was imposed because the amplitude ratio is an exponential function of $L/D_p$, and although amplitude ratios greater than 500 could be measured, at low flow rates and high $L/D_p$ the amplitude ratio could be even greater at the frequencies required. For the 0.03935-in. particles, several runs using two different bed depths, 0.51 and 0.29 in., were made with identical flow rates and only slightly differing void fractions.

Mass flow rates varied from 700 to 96,400 lb./(hr.) (sq.ft.) and Reynolds numbers from 23.4 to 18,200. Measurements averaged for at least three different frequencies were used to obtain a heat transfer coefficient for each flow rate and as many as ten different frequencies were used in some cases. Deviations from the average were always less than 3%. A total of three hundred forty nine experimental runs were made and from the results fifty heat transfer coefficients were obtained.

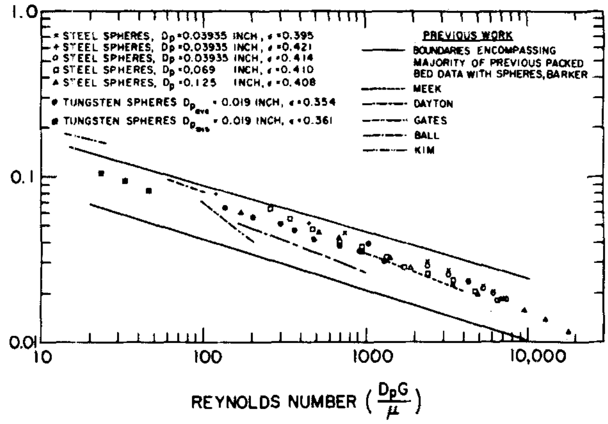


Fig. 5. Comparison of experimental data with prior data.

## DISCUSSION: PACKED BEDS

Most of the heat transfer coefficients were calculated using the amplitude ratio and Equation (3). Periodic calculations using the phase lag in conjunction with Equation (4) were made and the results were compared with those obtained for the same flow rate from the amplitude ratio. Agreement to within 5% was always obtained.

At very low Reynolds numbers (less than 100) experimental amplitude ratios obtained were questionable because at the high frequencies needed the amplitude ratios were too small to measure accurately. In these particular experiments, heat transfer coefficients were obtained from phase angle measurements in conjunction with Equation (4), to avoid the need for very thin beds.

Experimental results plotted in Figure 4 as heat transfer coefficient vs. mass velocity show that for any particular flux $h$ increased as some power of the mass velocity. For the steel spheres of uniform diameter, $h$ is proportional to $G^{0.60}$. For the tungsten spheres of nonuniform diameter, $h$ is proportional to $G^{0.66}$. Results of the two sets of experiments using 0.0395-in. steel spheres and identical mass flow rates but with void fractions of 0.395 and 0.414 indicate that the effect of bed depth is small. The maximum difference of 11% may be related to void fraction, $L/D_p$ or both.

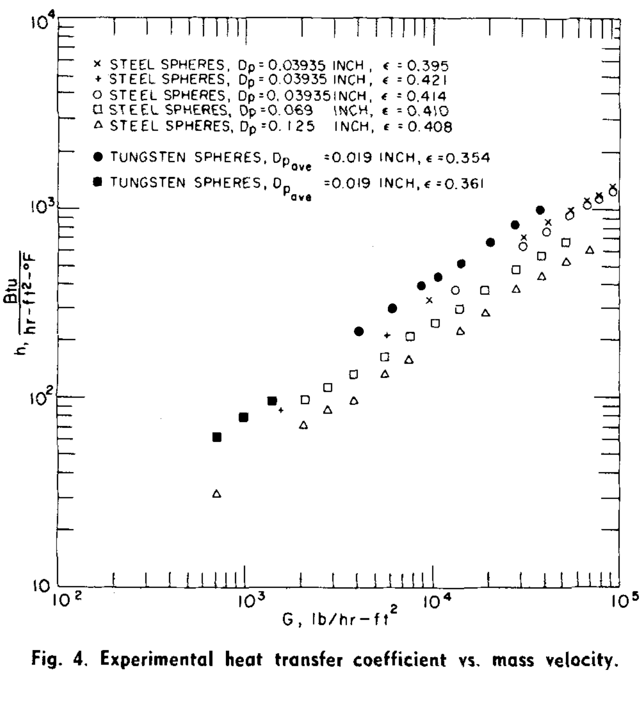


Fig. 4. Experimental heat transfer coefficient vs. mass velocity.

Two sets of experiments were made at identical mass velocities and almost identical void fraction and $L/D_p$ using particle sizes of 0.069 and 0.125 in. From these experiments $h$ was found to vary as $D_p^{-0.44}$.

The experimental results plotted in Figure 5 as $\varepsilon j_h$ vs. $N_{Re}$ for different particle sizes at very high mass flow rates agree within 10% of a best-by-sight line. The solid lines in Figure 5 are the approximate upper and lower boundaries of packed bed particle-to-fluid heat transfer coefficient data for spheres compiled by Barker (*1*). The experimental results obtained in the present investigation lie in the upper range of this data. It can be noted that the results using tungsten spheres of mixed particle sizes are slightly lower than most of the other results using uniform particle size. Possibly the difference in arrangement affects the heat transfer apart from the effect of bed porosity but there isn't sufficient evidence to determine if this is indeed so. The other lines are plotted from results obtained by other experimenters using the cyclic heating method. The results of Meek (*9*) are based on more than two hundred runs in which special precautions were taken to eliminate wall effects. Dayton et al. (*6*) did not include the bed void fraction in their report and in the plot of their data in Figure 4, an ε of 0.40 is assumed. Gates (*11*) reported results of four experiments, but he reports his beds had void fractions in excess of the 0.476 obtained in cubical packing. Kim (*10*) reported two values of heat transfer coefficient and Ball (*8*), four. Although none of the previous studies covered as wide a range of conditions as those in the present investigation, results of the various studies show good agreement. At $N_{Re}$ greater than 100, results of the present investigation are slightly above previous investigations. At lower $N_{Re}$, these results are lower than those of Kim (*10*) and Ball (*8*).

## EXPERIMENTAL RESULTS: FLUIDIZED BEDS

Sixty-two experiments were performed with air and helium as the fluidizing gases in particulate beds of 0.0394 in. diameter uniform lead spheres and 0.019 in. average diameter tungsten spheres. The particulate beds were shallow with a minimum packed $L/D_p$ of 5 and a maximum packed $L/D_p$ of 7, because the amplitude ratio decreased rapidly with increasing $L/D_p$ to the point where it could not be accurately determined. This problem was encountered by Kim (*10*) and Littman and Stone (*12*). As a check on the

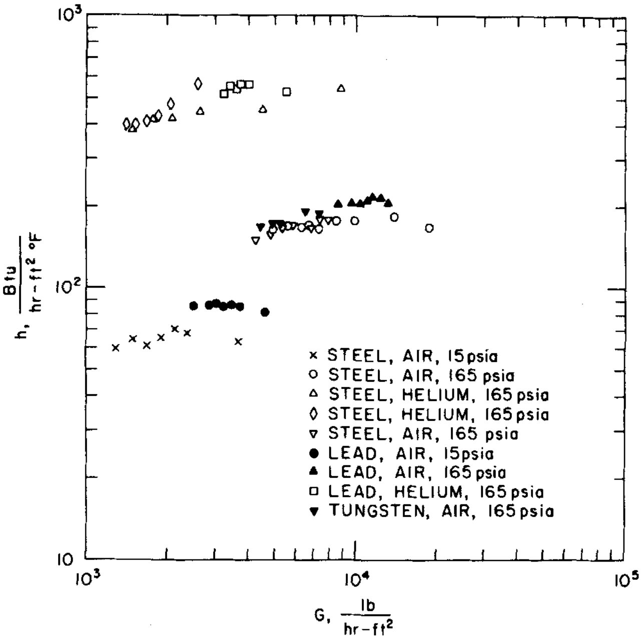


Fig. 6. Experimental heat transfer coefficient vs. mass flow rate.

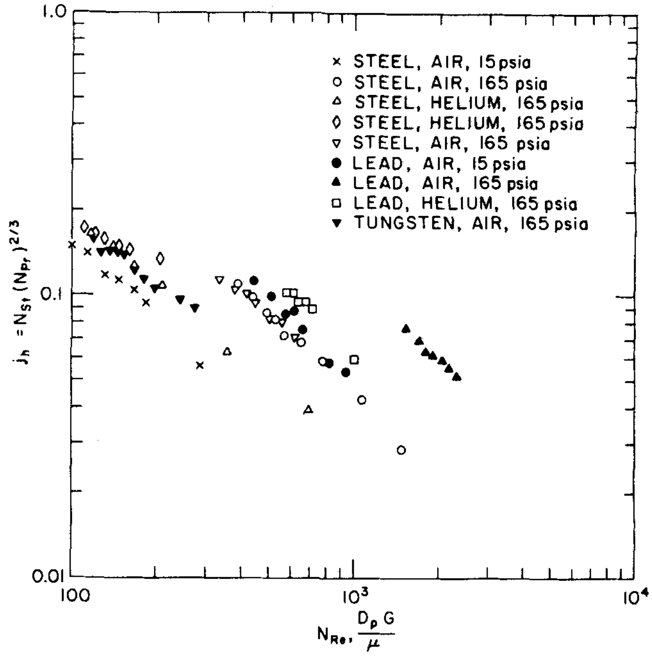


Fig. 7. Variation of $j_h$ with Reynolds number in fluidized-bed experiments.

method, experiments were performed with two bed depths using identical steel spheres and helium and air at 165 psig; one bed weighed 19.81 gm and the other bed weighed 14.84 gm. No significant variation of heat transfer coefficient was obtained with bed depth.

Results are given in Table 2.* Heat transfer coefficients shown are averages obtained for runs at three or more frequencies. In one experiment, deviation from the average heat transfer coefficient for the fluidized beds was as high as 15% but in almost all other experiments it was less than 5%.

Figure 6 shows the variation of heat transfer coefficient $h$ with mass velocity $G$. Heat transfer coefficients ranged from 60.2 to 566 B.t.u./(hr.)(sq. ft.) (°F.), mass velocities ranged from 1,290 to 19,000 lb./(hr.)(sq. ft.), and $N_{Re}$ ranged from 101 to 2,300. $G/G_{mf}$ was as high as 5.94. In this range of $G$ and of $N_{Re}$ there are little prior data on particle-to-fluid heat transfer coefficients for fluidized beds. In almost every instance, for a particular bed, increasing the flow rate had only a slight effect on the heat transfer coefficient. The sole exception was found in one experiment with a 14.84 g. bed of steel spheres fluidized with helium at 165 lb./sq.in.abs. at a mass velocity of 2,660 lb./(hr.)(sq.ft.) (see ◊ in Figure 6). Except for that one experiment, heat transfer coefficients obtained in the two different beds of identical steel spheres agreed very well at approximately the same mass velocity.

The observation that heat transfer coefficients in these fluidized-bed experiments was independent of mass velocity is contrary to packed-bed experience. Most authors disagree on the dependence of $h$ with mass velocity in fluidized beds, and previously, Wamsley and Johanson (*13*), Bradshaw and Myers (*14*), and Chang and Wen (*15*) are the only experimenters to report the independence of heat transfer coefficients with $G$. Other experimenters have determined that $h$ varies with $G$ to some power between 0.5 to 2.1.

Figure 7 is a plot of $j_h = N_{St} \times (N_{Pr})^{2/3}$ vs. $N_{Re}$. A straight line can easily be drawn through the data obtained for each set of experiments and each line has approximately the same slope. Except for the experiments with identical steel spheres at two different bed depths with the same flow rates, there is no agreement between sets of experiments.

The experiments were performed over a range of mass velocities which included the minimum fluidization velocity. Minimum fluidization was assumed to occur at the lowest flow rate for which steady particle motion could be observed. At low pressure, the values checked satisfactorily with the flow rate for minimum fluidization obtained from the plot of pressure drop vs. mass velocity. All minimum fluidization flow rates were in good agreement with the correlation of Wen and Yu (*16*).

Heat transfer coefficients obtained at minimum fluidization are plotted as $N_{St} \times (N_{Pr})^{2/3} \times (N_{Re})^{1/3}$ vs. $N_{Re}$ in Figure 8. The data of Bradshaw (*17*) and Chang and Wen (*15*) are also plotted in this figure. Figure 8 shows that $N_{St} \times (N_{Pr})^{2/3}$ at minimum fluidization varied as $(N_{Re})^{-1/3}$. This suggested that heat transfer coefficients in the fluidized beds at minimum fluidization could be related to heat transfer coefficients in a packed bed shown in Figure 5. Except for the nonuniform tungsten spheres, the heat transfer coef-

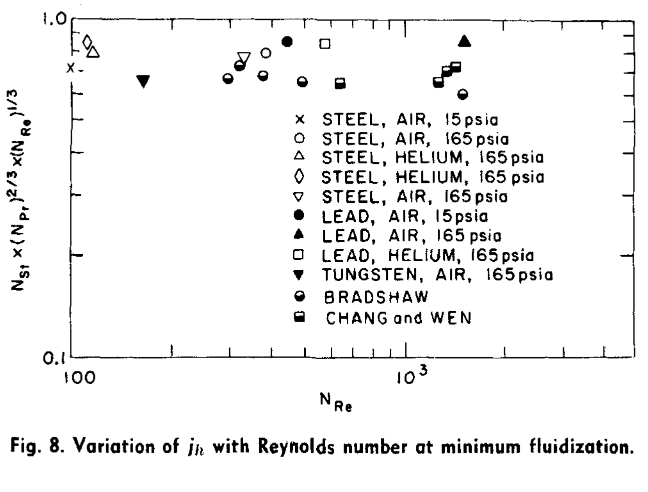


Fig. 8. Variation of $j_h$ with Reynolds number at minimum fluidization.

*See footnote on page 1183.

ficients obtained at minimum fluidization agreed to within 10% of the average values obtained from Figure 5. The coefficient for the nonuniform tungsten spheres was about 15% less than this average value. The heat transfer coefficients at minimum fluidization of Bradshaw (*17*) and Chang and Wen (*15*) were also compared with the packed-bed data of Figure 5. Their data were generally lower than the experimental data plotted in Figure 5, the maximum deviation being approximately 25%. In all cases, their data were above the lower solid line of Figure 5. This indicates that the heat transfer coefficients obtained at minimum fluidization were substantially the same as those obtained in packed beds. It may be concluded, therefore, that the heat transfer coefficients obtained for the fluidized beds in the present investigation were approximately equal to those which would be predicted for the same beds at minimum fluidization using a packed-bed correlation.

Chang and Wen (*15*) suggest that the independency of $h$ with $G$ may be explained by assuming that the bed can be approximated by a bed of uniformly suspended particles. Based on the assumption that the sum of the drag force, calculated as the drag on an isolated sphere, and buoyancy force on any particle is equal to the gravitational force, they derive the relationship for $500 < N_{Re} < 200{,}000$

$$N_{Nu} = 2 + 0.79\,(N_{Ar})^{1/4}\,(N_{Pr})^{1/3} \qquad (6)$$

which is independent of $G$. The agreement between heat transfer coefficients calculated with Equation (6) and those obtained in the present experiment is fair, the maximum difference being about 75%. The lack of good agreement is to be expected because the present experiments are not physically represented by the model of Chang and Wen (*15*), since the void fraction and hence the separation distance between particles are not extremely large. Wen and Yu (*15*) show that in a fluidized bed the assumption that the drag force and the buoyancy force on an isolated particle is equal to the gravitational force is only valid for large particle separations and is certainly not valid at or close to minimum fluidization.

All other prior experiments were performed with lower mass velocities and $N_{Re}$ than obtained in the present investigation, and serious objections were cited by Frantz (*3*) with respect to much of the data. Frantz (*3*) concluded that particle-to-fluid heat transfer coefficients were measured by only two groups of experimenters, Heertjes and McKibbins (*18*) and Walton et al. (*19*), and that the data of Heertje and McKibbons (*18*) were to be considered questionable because the temperature probe diameters were so large that the flow pattern was disrupted. A more recent paper by Juveland et al. (*20*) also presents particle-to-fluid heat transfer data but, again, in the low $N_{Re}$ range. The data of both Walton et al. (*19*) and Juveland et al. (*20*) show an increase in $h$ with $G$, whereas the results of the present experiments show no change of $h$ with $G$ and no correlation with their results.

## DISCUSSION OF SOURCES OF ERRORS

There are a number of possible sources of error in determining particle-to-fluid heat transfer coefficients which can arise if the assumptions made in deriving Equations (1) and (2) are not valid.

For the heat transfer process to be linear, it is sufficient that the temperature waves be sinusoidal with identical frequency at all positions in the bed and that the amplitude ratio and phase shift of the waves at a specified frequency be only a function of longitudinal position. Previous experiments by Dayton et al. (6), Meek (9), Kim (*10*), and Littman and Stone (*12*) indicated that these criteria are met. In the present study, experiments with the different bed depths of 0.0395-in. diameter spheres showed that the heat transfer coefficient was independent of bed depth which further confirmed this conclusion.

For a randomly packed bed of particles, the assumption of constant void fraction is acceptable provided the ratio of bed diameter to particle diameter is large. In the present study, this criterion was met in all experiments except when 0.125-in. diameter particles were used. The effect in these experiments is small since no significant difference in results was obtained with these spheres compared with smaller diameter spheres.

Errors can arise if the velocity profile is nonuniform because of a nonuniform entrance velocity or a wall effect, particularly if the gas temperature is measured with a resistance thermometer. A wall effect would be expected to occur in the packed bed with 0.125-in. diameter spheres and in the fluidized bed with 0.089-in. diameter spheres. If the coolant velocity adjacent to the test section walls is lower than at the center, an apparent attenuation occurs due to the fact that the coolant temperature near the wall lags that near the center. In addition, a nonuniform velocity profile causes a variation in heat transfer coefficient across the test section. For the packed bed, these errors were made negligible by: (1) ensuring that the velocity profile at the entrance of the bed was uniform by suitable design of the test sections; designing the resistance thermometers to respond primarily to temperatures in the center region of the cross section; and operating at velocities, frequencies, and bed depths such that the ratio of bed depth to temperature wave length was small.

The assumptions of constant and uniform bed void fraction and plug flow of gas are not really valid for a bubbling fluidized bed, but they have been used successfully by Kim (*10*) and Littman and Stone (*12*) in applying the cyclic heat transfer method to fluidized beds and by experimenters who determined $h$ by other methods.

Radial temperature gradients were minimized by designing the heater to produce a uniform temperature profile in the gas and by insulation of the test section. Attenuation of the temperature wave by the walls was expected to be small because of the high ratios of particle to wall surface area and the relatively low thermal conductivity of the Lucite. This conclusion was supported by the fact that during preliminary testing without the bed the upstream and downstream resistance thermometers measured identical temperature changes over the entire range of flows and frequencies used in these experiments which indicated that heat exchange with the wall was negligible. Although the wall to gas heat transfer coefficient would be substantially increased in the presence of the particulate bed, for the conditions of these experiments, the effect would remain small.

Bell and Katz (5) showed that by choosing sufficiently high frequencies, the amplitude ratio obtained experimentally for infinite $K_e$ could be made equal to that with $K_e = 0$. Thus the heat transfer coefficient obtained would be independent of $K_e$. Fortuitously, the frequencies required in this case are the same as those necessary to obtain minimum errors in the use of the cyclic temperature method and they were used for almost all the packed-bed experiments and as many as possible fluidized-bed experiments. The errors due to gas mixing are minimized because of small effective conductivity and high gas velocity, the high velocities resulting in long temperature wavelength compared with the bed depth.

The important physical properties are density and specific heat of the fluid and particles and viscosity of the fluid. The change in properties is small provided that small temperature amplitude changes and pressure drops through the bed are used, and the effect of such change on the heat transfer coefficient is negligible. To check the effect of varying physical properties, runs were made at the same flow rate with inlet amplitudes ranging from 1° to 20°F. and no variation in amplitude ratio or phase lag could be detected. Additional runs were made at pressures up to 100 lb./sq. in. abs. to vary the pressure drop at a number of flow rates and, similarly, no effect was observed.

The assumption of constant heat transfer coefficient throughout the bed is warranted provided that the bed voidage is constant and the velocity profile across the bed is uniform. Meek (9) found that errors due to temperature gradients in the particle are less than 1% for systems where $hD_p/k_s$ is less than 2. The present experiments were performed with steel balls, lead balls, and tungsten particles where $hD_p/k_s$ was always $\leq 0.5$ and hence the resulting errors were negligible.

Another source of error is the determination of the void fraction. Although void fraction does not enter into the determination of heat transfer coefficient obtained from the amplitude ratio at high frequencies, since

$$(1-\varepsilon)L = \frac{\text{wt. of spheres}}{\rho_s A} \tag{7}$$

it does enter into the evaluation of $\varepsilon j_h$. The void fraction was determined from measurements of the cross-sectional area bed depth, and particle weight using Equation (7). Maximum errors in determining void fraction are estimated to be 3%.

## CONCLUSIONS

Experiments on packed beds and fluidized beds of small diameter spheres at high mass velocities have shown that particle-to-fluid heat transfer coefficients can be satisfactorily determined with the cyclic temperature method provided that sufficiently high frequencies can be used. The errors arising in using this method can be made quite small by suitable choice of experimental equipment and operating parameters.

Experimental results for packed beds using particle diameters from 0.019 to 0.125 in. and mass velocities up to 96,400 lb./(hr.)(sq. ft.) were satisfactorily correlated within 10% as $\varepsilon j_h$ vs. $N_{Re}$ and compared favorably with results of other experimenters at much lower mass velocities and using larger particles. The particle-to-fluid heat transfer coefficient varied roughly with the 0.60 to 0.66 power of the mass velocity and decreased with increasing particle diameter. The maximum heat transfer coefficient obtained in these experiments was 1,310 B.t.u./(hr.)(sq. ft.)(°F.).

For fluidized beds heat transfer coefficients obtained at minimum fluidization were in good agreement with those obtained from using packed beds. Heat transfer coefficients obtained using particles with diameters ranging from 0.019 to 0.089 in. and with air and helium as the fluidizing gases were found to be essentially independent of fluid mass velocity and were approximately equal to the values obtained under conditions of minimum fluidication.


## ACKNOWLEDGMENT

The invaluable assistance of Matthew Rosso in constructing the test section and in performing the experiments and of John Jacobs in designing the electronics equipment is gratefully acknowledged.

This work was performed under the auspices of the U.S. Atomic Energy Commission.


## NOTATION

$A$ = flow area of test section, sq. ft.
$C$ = specific heat, B.t.u./(lb.)(°F.)
$D_p$ = particle diameter, ft.
$g$ = gravitational acceleration, sq. ft./hr.
$G$ = superficial fluid mass velocity, lb./(hr.)(sq. ft.)
$h$ = particle-to-fluid heat transfer coefficient, B.t.u./(hr.)(sq. ft.)(°F.)
$j_h = (N_{St})(N_{Pr})^{2/3}$
$K$ = thermal conductivity, B.t.u./(hr.)(ft.)(°F.)
$K_e$ = effective axial solids thermal conductivity, B.t.u./(hr.)(ft.)(°F.)
$L$ = bed length, ft.
$N_{Ar}$ = Archimedes number, $D_p^3 g\rho_g(\rho_g-\rho_g)\mu^2$, dimensionless
$N_{Nu}$ = Nusselt number, $hD_p/K$, dimensionless
$N_{Pr}$ = Prandtl number, $C\mu/K$, dimensionless
$N_{Re}$ = Reynolds number, $D_pG/\mu$, dimensionless
$N_{St}$ = Stanton number, $h/CG$, dimensionless
$T$ = temperature, °F.
$t$ = time, hr.
$V$ = interstitial velocity, ft./hr.
$X$ = longitudinal distance coordinate, ft.
$y = C_s\rho_s D_p\omega\varepsilon/6C_gG$
$\varepsilon$ = void fraction, cu. ft. voids/cu. ft. total bed
$\mu$ = viscosity, lb./(hr.)(ft.)
$\rho$ = density, lb./(hr.)(ft.)
$\phi$ = phase shift, rad.
$\omega$ = angular frequency of temperature oscillation, rad./sec.

### Subscripts

$g$ = gas
$Mf$ = minimum fluidization
$s$ = solid
1 = upstream
2 = downstream

## LITERATURE CITED


1. Barker, J. J., *Ind. Eng. Chem.*, 57, 43 (Apr. 1965).
2. *Ibid.*, 33 (May, 1965).
3. Frantz, J. F., *Chem. Eng. Progr.*, 57, 35 (July, 1961).
4. Schumann, T. E. W., *J. Franklin Inst.*, 280, 405 (Sept., 1929).
5. Bell, J. C., and E. F. Katz, paper presented at Heat Transfer and Fluid Mechanics Inst. Meeting, Berkeley, Calif. 243 (1949).
6. Dayton, R. W., S. L. Fawcett, R. E. Grimble, and C. E. Sealander, *Battelle Mem. Inst. Rept. No. BMI-747* (1952).
7. Dingee, D. A., and J. W. Chastain, *Battelle Mem. Inst. Rept. No. BMI-1167* (1957).
8. Ball, W. E., Ph.D. dissertation, Washington Univ., St. Louis, Mo. (1958).
9. Meek, R. M. G., *Intern. Develop. Heat Transfer*, Pt. IV, 770 (1962).
10. Kim, D. S., Ph.D. dissertation, Ohio State Univ., Columbus (1965).
11. Gates, L. E., M. S. thesis, Ohio State Univ., Columbus (1964).
12. Littman, Howard, and A. P. Stone, *Chem. Eng. Progr. Symp. Ser. No. 62*, 62, 47 (1966).
13. Wamsley, W. W., and L. N. Johanson, *Chem. Eng. Progr.*, 50, 347 (1954).
14. Bradshaw, R. D., and J. E. Myers, *AIChE J.*, 9, 590 (Sept., 1963).
15. Chang, T. M., and C. Y. Wen, *Chem. Eng. Progr. Symp. Ser. No. 67*, 62, 111 (1966).
16. Wen, C. Y., and Y. H. Yu, *Chem. Eng. Progr. Symp. Ser. No. 62*, 62, 100 (1966).
17. Bradshaw, R. D., Ph.D. thesis, Purdue Univ., Lafayette, Ind. (1961).
18. Heertjes, P. M., and S. W. McKibbins, *Chem. Eng. Sci.*, 5, 161 (1956).
19. Walton, J. S., R. L. Olson, and Octave Levenspiel, *Ind. Eng. Chem.*, 44, 1474 (1952).
20. Juveland, A. C., H. P. Deinken, and J. E. Dougherty, *Ind. Eng. Chem. Fundamentals*, 3, 329 (Nov. 1964).



*Manuscript received October 14, 1966; revision received April 20, 1967; paper accepted May 1, 1967.*